Journal of Colloid and Interface Science 330 (2009) 156–162

Contents lists available at ScienceDirect

Journal of Colloid and Interface Science

www.elsevier.com/locate/jcis

A new insight on the dynamics of sodium dodecyl sulfate aqueous micellar solutions by dielectric spectroscopy

Leandro Lanzi [a], Marcello Carlà [a], Leonardo Lanzi [a], Cecilia M.C. Gambi [a,b,*]

[a] Department of Physics, University of Florence and CNISM, Via G. Sansone 1, 50019 Sesto Fiorentino (Florence), Italy
[b] CRS-Soft Matter (CNR-INFM) Università di Roma "La Sapienza," P.le A. Moro 2, 00185 Rome, Italy

ARTICLE INFO

Article history:
Received 19 March 2008
Accepted 16 October 2008
Available online 22 October 2008

Keywords:
Micellar solution
Dielectric spectroscopy
Relaxation times
Bound water

ABSTRACT

Aqueous sodium dodecyl sulfate micellar solutions were investigated by a recently developed double-differential dielectric spectroscopy technique in the frequency range 100 MHz–3 GHz at 22 °C, in the surfactant concentration range 29.8–524 mM, explored for the first time above 104 mM. The micellar contribution to dielectric spectra was analyzed according to three models containing, respectively, a single Debye relaxation, a Cole–Cole relaxation and a double Debye relaxation. The single Debye model is not accurate enough. Both Cole–Cole and double Debye models fit well the experimental dielectric spectra. With the double Debye model, two characteristic relaxation times were identified: the slower one, in the range 400–900 ps, is due to the motion of counterions bound to the micellar surface (lateral motion); the faster one, in the range 100–130 ps, is due to interfacial bound water. Time constants and amplitudes of both processes are in fair agreement with Grosse's theoretical model, except at the largest concentration values, where interactions between micelles increase. For each sample, the volume fraction of bulk water and the effect of bound water as well as the conductivity in the low frequency limit were computed. The bound water increases as the surfactant concentration increases, in quantitative agreement with the micellar properties. The number of water molecules per surfactant molecule was also computed. The conductivity values are in agreement with Kallay's model over the whole surfactant concentration range.

1. Introduction

Understanding the physicochemical properties of self-assembling processes of amphiphilic molecules in aqueous solution is relevant in basic and applied research [1–3]. Surfactant micelles in aqueous solutions have been studied carefully from the point of view of structure and interactions since the pioneering work of Ref. [4], not only because of the numerous applications in pharmacological, chemical and biochemical industries but also as model systems. In fact, more complex structures in aqueous solution like oil in water microemulsions (also called swollen micelles), vesicles (or bilayer micelles), phospholipid membranes and proteins in solution share with the micellar solutions the same interfacial region between the aggregates and the aqueous dispersing medium. In case of ionic species there is also a Gouy–Chapman layer whose extension is measured by the Debye screening length [5]. Presence of surface charges on both self-assembling aggregate and diffuse layer are common features for the above mentioned structures.

More recently, thanks to technological improvements, it has been possible to study experimentally the dynamical processes occurring in aqueous micellar solutions in a broad frequency range; theoretical studies have been advanced as well on this subject.

Dielectric spectroscopy has proven a powerful tool to investigate in details the dynamical processes of micellar solutions, due to its sensitivity to all kind of dipole moment fluctuations. This technique can monitor processes spanning from reorientation of water molecules and of stable ion pairs [6,7], to fluctuations of instantaneous dipole moments due to polarization of the ions surrounding the charged micelles, either the more tightly bound interfacial counterions and the less bound ones in the diffuse layer [8].

Summarizing the results in the literature, we cite first the improvements operated by Grosse in modeling charged particles in aqueous electrolytical solutions [9,10]. At variance with previous theories [11] that considered only a thin ionic layer, Grosse introduced a thick diffuse layer surrounding the charged particles. Schwarz's model [11] led to consider only the conduction of the counterions along the micellar surface (lateral motion), described by a single low-frequency relaxation process. On the contrary, the addition of diffusion of ions in the bulk electrolyte introduced by Grosse's model (radial motion) was able to predict the high dielectric amplitudes at low frequency as well as the relaxation times observed experimentally. Relaxations due to lateral and radial motion appear well separated in frequency when the radius of the

* Corresponding author.
E-mail address: gambi@fi.infn.it (C.M.C. Gambi).

0021-9797/$ – see front matter
doi:10.1016/j.jcis.2008.10.039

charged particle is much greater than the Debye screening length. Two relaxation processes were predicted, one at lower frequency (tens of MHz) due to the fluctuations of the diffuse ion cloud surrounding the particle; the other at higher frequencies (hundreds of MHz), due to the lateral or tangential interfacial polarization at the micelle/solvent boundary (the latter process was also modeled by Pauly and Schwan in [12]). Counterions diffusing in the bulk solution are less mobile than those moving at the surface by the conduction mechanism. A summary of Grosse's theory is reported in [13].

Micellar solutions without added salt were studied in [14] in the frequency range 1 MHz–30 GHz, taking into account the radial extension of a diffuse layer due to the dissociated counterions whose density was considered a radial function of the distance from the micelle surface. The range where the surfactant aggregates and their ionic clouds play an active role was found below 3 GHz. A Debye relaxation process and a Cole–Cole one were used to model the micellar system with five fitting parameters, keeping fixed at the values of pure water only the high frequency dielectric constant and the relaxation time, 5.3 and 8.3 ps respectively, at 25 °C. CTAB (hexadecyltrimethylammonium bromide) and SDS (sodium dodecyl sulfate) aqueous micelles (composed by cationic and anionic surfactants, respectively) were investigated at concentrations 10–20 mM and 20–60 mM, respectively. The model in [14] takes into account the charge of the micelle and the finite thickness of the layer surrounding the micelle; the polarization mechanism is associated with the lateral diffusion of the Gouy–Chapman layer counterions. This model justifies the relaxation in the frequency region of hundreds of MHz.

In agreement with Grosse's theory, in papers [8,15] on cationic surfactant micelles, two micelle-specific relaxations were found. The process with the lower relaxation time was attributed to the radial motion of the diffuse ion cloud around the micelle, whereas the faster relaxation was interpreted as due to a rotation of stable ion pairs or a hopping of counterions bound to the charged surface of the micelle (lateral motion). Analysis of the water contribution to the complex dielectric constant revealed that the charged head groups are strongly hydrated with a presence of water molecules bound to polar heads and counterions; even below the hydrophilic interfacial layer, strongly bound or irrotational water is trapped in proximity of the micellar core. Five Debye relaxation processes were used to analyze the dielectric spectra.

In [16,17] SDS micellar solutions were studied at concentrations from 0.018 to 0.104 M by Broad Band Dielectric Spectroscopy (BBDS) [18]. The spectra exhibit two relaxation processes at 30 MHz and 200 MHz due to the micellar contribution, a relaxation process at 18 GHz due to the solvent and a further process at 1.8 GHz attributed to water molecules in a micelle hydration layer (interfacial or bound water). Most of water has the relaxation time of pure water (8.3 ps); a small fraction of water is characterized by a reduced mobility (120 ps relaxation time). No irrotational water due to strong solute–solvent interactions was found, at variance with previously described cationic systems that showed considerable irrotational bonding.

It has to be stressed that the number of relaxation processes due to the micelles and their interpretation is still a matter of discussion.

The object of the present work is the investigation of the dielectric properties of two components aqueous ionic micellar solutions (SDS and water), with SDS concentration below, close and well above the maximum concentration explored up to now. Precisely, this paper covers the concentration range 29.8–524 mM, completing and extending our previous works [19,20].

The extended concentration range allows the investigation of the relaxation processes with both dilute (non-interacting) and concentrated (interacting) micelles. At our knowledge, no previous work extends above the concentration 104 mM studied in [16,17].

Measurements have been performed on the frequency range 100 MHz–3 GHz using the new Double Differential Dielectric Spectroscopy (DDDS) technique that we have developed a few years ago [20–22].

2. Micellar solutions model

Micelles are aggregates of molecules endowed with a hydrophobic tail, mainly located in the core of the micelle, and a hydrophilic polar head at the interface with the aqueous dispersing phase. In the case of SDS, the surfactant polar head is composed by the sulfate group with one negative charge and by the positive sodium counterion. Counterions are partially bound to the heads, partially dispersed in the diffuse layer. We can distinguish among three concentric spherical shells: (a) the hydrophobic core of the micelle; (b) the interfacial layer in which polar heads, some counterions and water molecules (bound water) are located; (c) the diffuse layer (or ion cloud) with the remaining unbound counterions in the aqueous phase (bulk water). We name micelle the sum of core (a) and interfacial shell (b), as in the two-shell model of the Small Angle Neutron Scattering (SANS) literature [23–27]. Hence, the micelle is a negatively charged particle surrounded by a positively charged region (c), whose extension is measured by Debye's length l_D [5].

The micellar shape is spherical with radius R at low surfactant concentration and ellipsoidal with maximum axial ratio 1.3 at higher concentration [26]. In the latter case, R is the radius of the sphere having a volume equivalent to that of the ellipsoid.

According to Grosse's model, the single micelle can be considered a dielectric sphere of dielectric constant ϵ_p, with surface charge $Qe = -\alpha Ne$, where N is the average aggregation number (number of surfactant molecules per micelle), $\alpha = Q/N$ is the fractional ionization, namely the fraction of unbound counterions dispersed in the diffuse layer (c) and e is the electron charge. Q is the number of negative charges on the micelle, d is the interfacial shell thickness.

The micelles are dispersed in a medium of dielectric constant ϵ_m and conductivity k_m.

The interaction among micelles is described by the Hayter–Penfold potential [23,24] that takes into account the hard sphere and the Coulombic repulsion between negatively charged micelles screened by the presence of the unbound positive counterions of the diffuse layer.

Whereas the SDS micellar structure and interactions are well known, the dynamic properties of the micelles are not yet completely understood.

3. Experimental

3.1. Materials

Micellar solutions of SDS ($C_{12}H_{25}SO_4^-Na^+$) in water were prepared with surfactant concentrations $c = 29.8$ mM, 134.9 mM, 259.9 mM, 524 mM, all above the critical micellar concentration cmc = 8.1 mM at 22 °C. The aqueous phase in which micelles are dispersed is composed of water and dissociated surfactant molecules in the monomeric state at the cmc. SDS was from BDH, England (purity 99%). Water was from a Millipore Milli-Q apparatus.

3.2. Method

Measurements have been performed at temperature $T = 22.0 \pm 0.5$ °C using an Anritsu MS4661A Vector Network Analyzer (VNA)

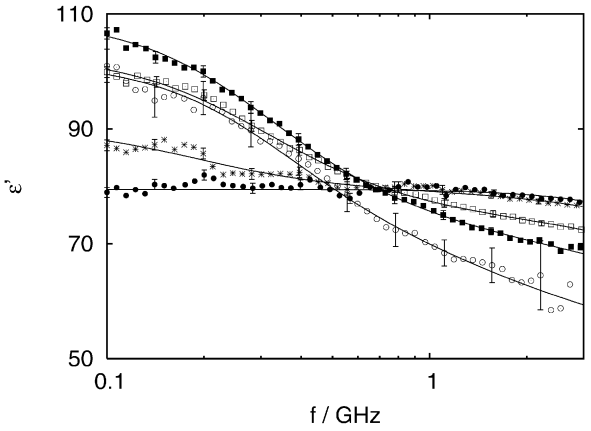

Fig. 1. Experimental spectra vs frequency: ε' of water (black points) and of SDS micellar solutions at concentrations 29.8 mM (stars), 134.9 mM (squares), 259.9 mM (black squares) and 524 mM (circles). The error bars are standard deviations in this and all following figures. Here, the errors are reported for water and only for $c = 29.8$ mM and 524 mM for clarity of the drawings. The continuous lines for micellar solutions are the plot of the best fit with the DD model. The continuous line for water represents the calculated values using the parameters known from literature (see Section 4.1).

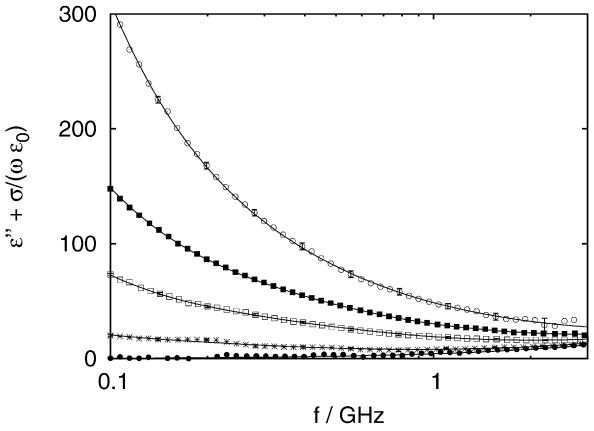

Fig. 2. Experimental spectra vs frequency: $\varepsilon'' + \sigma/(\omega\varepsilon_0)$ of water (black points) and of SDS micellar solutions at concentrations 29.8 mM (stars), 134.9 mM (squares), 259.9 mM (black squares) and 524 mM (circles). The error bars are standard deviations in this and all following figures. Here, the errors are reported for water and only for $c = 29.8$ mM and 524 mM for clarity of the drawings. The continuous lines for micellar solutions are the plot of the best fit with the DD model. The continuous line for water represents the calculated values using the parameters known from literature (see Section 4.1).

and a new double-differential method based on cells built as a coaxial transmission line. The details of the experimental technique, the calculation procedure and the drawing of the cells can be found in [20–22]. A summary of the new method is reported in Appendix A.

The explored frequency range was from 100 MHz to 3 GHz, with 500 logarithmically spaced points. The nominal impedance of the empty coaxial cell was 50 Ω and the signal intensity 0 dBm for all measurements.

In brief, the micellar solution was put into the cell and the cell was connected to the VNA at both ends. The VNA sent a signal to the cell and measured the reflected and the transmitted signals. Two cells of different length were used for each sample, both empty and filled with the sample in order to subtract the cell contribution. The complex dielectric permittivity $\hat{\varepsilon} = \varepsilon' - j\varepsilon''$ (where $j^2 = -1$) vs frequency f together with the low frequency limit of conductivity σ were obtained for each sample.

The fit with the model functions described in next paragraph were performed with the MINUIT procedure from the CERN library. In order to take into account both real and imaginary part of $\hat{\varepsilon}$, an auxiliary real function was built defined as $\varepsilon'(f)$ in the base frequency interval and as $\varepsilon''(f)$ in a second shifted not overlapping frequency interval. Each value in the auxiliary function was associated a weight according to the instrumental and procedural errors.

4. Results

Figs. 1 and 2 show the real and imaginary parts of the complex dielectric permittivity of the SDS micellar solutions and of pure water. Points are experimental data, lines are the results of the fits as described below.

4.1. Bulk water spectrum

The dielectric behavior of bulk water, known from the literature, is characterized by two relaxation processes with time constants of ∼1 ps and ∼8 ps [29]. The first one is due to the reorientation of free water molecules and is well above our frequency range; the second is due to the relaxation of the water hydrogen-bond network and is clearly visible in the water spectrum of Figs. 1 and 2 as a decrease of the real part of permittivity and an increase of the imaginary part, in the 1–3 GHz frequency range.

The bulk water behavior due to the hydrogen-bond network is well described by a Debye relaxation process [29]:

$$\hat{\varepsilon}_w(\omega) = \varepsilon_\infty + \frac{\Delta\varepsilon_w}{1 + j\omega\tau_w}, \tag{1}$$

where $\omega = 2\pi f$ is the angular frequency, $\Delta\varepsilon_w$ is the relaxation amplitude (or step) and τ_w is the relaxation time constant; ε_∞ is the water permittivity at ω above $1/\tau_w$ and accounts also for the contribution of free water molecules, as reported in [30].

Values of $\Delta\varepsilon_w$, τ_w and ε_∞ cannot be obtained with any reasonable accuracy from our data for pure water, due to the limited frequency range, but only the sum $\Delta\varepsilon_w + \varepsilon_\infty$. This value, 79.59 ± 0.03 [22], compares well with the value 79.45 in [30]. This is shown in Figs. 1 and 2, where the lines corresponding to pure water data are computed using the literature values. Hence for all subsequent calculations we have used the values $\tau_w = 8.93$ ps, $\varepsilon_\infty = 5.72$ and $\Delta\varepsilon_w + \varepsilon_\infty = 79.45$ obtained from Eqs. (3)–(5) in Ref. [30] at 22 °C.

4.2. Micellar solutions spectra

Experimental data have been analyzed according to three commonly used models [31] to account for the contribution of the micellized solute. The first model is obtained adding a single Debye relaxation process to the water model described above (SD model). The whole expression of the dielectric permittivity with the SD model is

$$\hat{\varepsilon}(\omega) = \phi\left(\varepsilon_\infty + \frac{\Delta\varepsilon_w}{1 + j\omega\tau_w}\right) + \frac{\Delta\varepsilon}{1 + j\omega\tau} + \frac{\sigma}{j\omega\varepsilon_0}, \tag{2}$$

where ϕ is the volume fraction of water that behaves as bulk water (hence, excluding interfacial water), $\Delta\varepsilon$ and τ are respectively the step and the relaxation time due to micelles, ε_0 is the vacuum permittivity and σ is the low frequency limit conductivity.

In the second model, the second term of Eq. (2), namely the Debye relaxation that accounts for the micelles effect, is replaced by a Cole–Cole relaxation, introducing, with the new parameter h, a spread into the relaxation time (CC model):

$$\hat{\varepsilon}(\omega) = \phi\left(\varepsilon_\infty + \frac{\Delta\varepsilon_w}{1 + j\omega\tau_w}\right) + \frac{\Delta\varepsilon}{1 + (j\omega\tau)^{1-h}} + \frac{\sigma}{j\omega\varepsilon_0}. \tag{3}$$

Table 1
Results of the fits of complex dielectric permittivity spectra by single Debye, Cole–Cole and double Debye models.

Model	c (mM)	ϕ	σ (Ω^{-1} m^{-1})	$\Delta\varepsilon$	τ (ps)	h	$\Delta\varepsilon'$	τ' (ps)	χ^2
Single Debye	29.8	0.9889 ± 0.0008	0.091 ± 0.001	10.6 ± 0.2	670 ± 20				1.1
	134.9	0.9336 ± 0.0005	0.3653 ± 0.0009	27.5 ± 0.1	443 ± 3				1.2
	259.9	0.8825 ± 0.0006	0.7808 ± 0.0009	36.9 ± 0.1	396 ± 2				1.2
	524	0.782 ± 0.003	1.685 ± 0.003	37.9 ± 0.4	328 ± 6				1.2
Cole–Cole	29.8	0.9850 ± 0.0008	0.085 ± 0.001	13.3 ± 0.5	850 ± 40	0.10 ± 0.01			1.0
	134.9	0.9250 ± 0.0009	0.355 ± 0.001	30.9 ± 0.4	492 ± 7	0.067 ± 0.006			1.0
	259.9	0.857 ± 0.001	0.758 ± 0.001	45.2 ± 0.5	469 ± 6	0.119 ± 0.005			1.0
	524	0.72 ± 0.01	1.663 ± 0.004	48 ± 2	350 ± 10	0.15 ± 0.02			1.0
Two Debye	29.8	0.9843 ± 0.0008	0.087 ± 0.001	10.9 ± 0.3	840 ± 30		1.2 ± 0.1	120 ± 10	1.0
	134.9	0.9258 ± 0.0009	0.358 ± 0.001	26.2 ± 0.3	522 ± 8		3.1 ± 0.3	130 ± 10	1.0
	259.9	0.861 ± 0.002	0.768 ± 0.001	34.6 ± 0.3	497 ± 7		6.2 ± 0.3	108 ± 7	1.0
	524	0.726 ± 0.006	1.672 ± 0.003	31.9 ± 0.6	440 ± 10		12.2 ± 0.9	100 ± 3	1.0

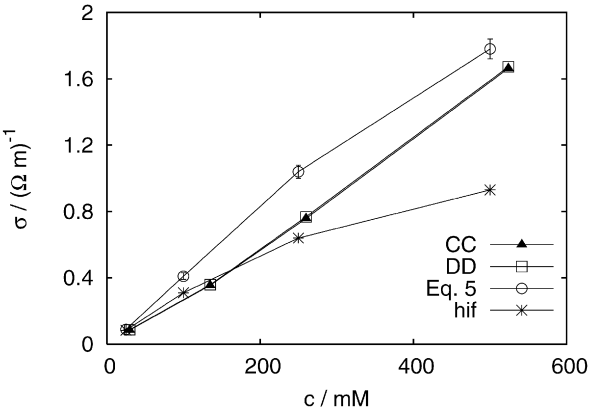

Fig. 3. Experimental low frequency conductivity σ vs concentration c. Triangles and boxes are values for the Cole–Cole and Double Debye models, respectively; open circles are the values obtained from Eq. (5) using the SANS data in Table 2; stars are the values calculated taking into account also the hydrodynamic interaction factor [35].

In the third model, the same term is split into two Debye relaxation processes, with the additional process characterized by step and time constant $\Delta\varepsilon'$ and τ' (DD model):

$$\hat{\varepsilon}(\omega) = \phi\left(\varepsilon_\infty + \frac{\Delta\varepsilon_w}{1 + j\omega\tau_w}\right) + \frac{\Delta\varepsilon}{1 + j\omega\tau} + \frac{\Delta\varepsilon'}{1 + j\omega\tau'} + \frac{\sigma}{j\omega\varepsilon_0}. \quad (4)$$

The parameters that appear in each model have been determined by a fit of experimental data with each one of Eqs. (2)–(4); results are reported in Table 1.

Lines in Figs. 1 and 2 for concentrations different from pure water are the plot of Eq. (4) with the parameters values obtained from the fit. The errors are standard deviations.

The χ^2 value is also reported in Table 1. The χ^2 value is higher for the SD model for all the samples, indicating that this model is less suitable to cope with the experimental data. On the contrary, the CC and the DD models give $\chi^2 = 1$.

In Fig. 3 the values of σ as a function of surfactant concentration are reported as obtained with the CC and DD models; for comparison, values computed as reported in [32] are shown:

$$\sigma = e^2 N_A\left[(u_{Na^+} + u_{DS^-})\text{cmc} + \left(\alpha u_{Na^+} + N\alpha^2 u_M\right)(c - \text{cmc})\right]. \quad (5)$$

In this equation N_A is the Avogadro number, $u_{Na^+} = 3.24 \times 10^{11}$ s kg^{-1} is the Na^+ mobility [33], $u_{DS^-} = 1.48 \times 10^{11}$ s kg^{-1} is the DS^- (dodecyl sulfate ion) mobility [34] and u_M is the mobility of the micelle with total radius R. From Stokes' law $u_M = (6\pi\eta R)^{-1}$, where η is the water viscosity ($\eta = 0.955$ cps at 22 °C [33]). The fractional ionization α, the average aggregation number N and the micelle radius R are available at 25 °C from the SANS study [26] and are reported in Table 2.

Table 2
Data from small angle neutron scattering for SDS aqueous micellar solutions at 25 °C [26].

c (mM)	R (10^{-10} m)	α	N
25.0	22.5	0.181	69.8
100.0	23.3	0.286	80.4
250.0	24.6	0.283	94.5
500.0	25.7	0.251	106.3

Of note, the first term between square parentheses takes into account the contribution of free surfactant monomers in water (both positive and negative charges); the second is due to micelle and diffuse layer contributions.

5. Discussion

In the dielectric spectroscopy literature on SDS micellar solutions at concentrations below 104 mM it is accepted that two relaxation processes arise from fluctuations of charges at the micelle–aqueous phase interface with relaxation times of 5.5 ns and 500 ps, respectively [16,17]. This interpretation agrees with Grosse's theory [9,10,13]. In this frame, the two relaxations are due to the radial charge fluctuations of the diffuse layer and to the lateral conduction of the counterions bound to the micellar surface. They are named by Grosse delta and gamma relaxations, and occur in the MHz and GHz ranges, respectively. According to [16,17] the lateral process is due to the reorientation of stable ion pairs or the hopping of counterions bound to the micellar charged surface between neighboring head groups, both for cationic and anionic SDS micellar solutions. In [16,17] a very wide frequency range (5 MHz–89 GHz) makes it possible to distinguish four relaxation processes. The fastest one, with time constant 8.93 ps, coincides with the hydrogen bond network relaxation of bulk water (see Section 4.1); a slower process (120 ps) is attributed to interfacial bound water. The further two processes, with time constant 500 ps and 5.5 ns, are of micellar origin.

In this work, all experimental data have been interpreted considering only two relaxation processes, with the SD and CC models, or three processes with the DD model. In all cases the fastest relaxation is due to the hydrogen bond network and its parameters $\Delta\varepsilon_w$, τ_w and ε_∞ have been kept fixed as explained in Section 4.1. Both anionic (SDS) and cationic alkyltrimethylammonium halides (C_nTAX) aqueous micellar spectra show the 8.93 ps relaxation process in the high frequency range [8,15].

In the SD and CC models, the second relaxation results to have a time constant in the 300–900 ps range, corresponding to a Grosse's gamma relaxation; when data are fitted considering a further relaxation (DD model), the time constant of the latter is in the range 100–130 ps and corresponds to the interfacial bound water relaxation, already described in [8,15,16].

Our data in Table 1, in particular σ, $\Delta\varepsilon$ and τ at $c = 29.8$ mM and 22 °C obtained with the CC model are in good agreement with those of Ref. [14], obtained with the same model, where $\sigma = 0.125\ \Omega^{-1}\,m^{-1}$, $\Delta\varepsilon = 13.6$, $\tau = 910$ ps and $h = 0.31$.

The comparison of our data with those of Ref. [16], in which a sum of 4 Debye relaxation processes is used, shows a fair agreement for the two common relaxation processes if one takes into account that the concentrations $c = 25$ mM and $c = 104$ mM in [16] are lower than ours $c = 29.8$ mM and $c = 135$ mM and that the temperature 25 °C is higher than our 22 °C. Actually, in [16] the authors report $\Delta\varepsilon = 4.08$, $\tau = 463$ ps, $\Delta\varepsilon' = 0.95$, $\tau' = 158$ ps at 25 mM, and $\Delta\varepsilon = 20.73$, $\tau = 537$ ps, $\Delta\varepsilon' = 2.58$, $\tau' = 96$ ps at 104 mM. Only the value of τ differs significantly (840 ps at 29.8 mM).

After this comparison, we assume that also at surfactant concentration higher than 104 mM the relaxation processes are of the type observed below 104 mM. The delta relaxation process was not considered in this work because it is too small in the explored frequency range. In fact, in [16,17], parameters values for this process are $\tau_\delta = 5.7$ ns and $\Delta\varepsilon_\delta = 3.36$ at 104 mM; this corresponds to a 3% effect at the low frequency end of the explored range (100 MHz). Furthermore, the h value of the CC model obtained in this work is very low, indicating presumably a small polydispersity of the relaxation processes or a sum of two relaxation processes, one largely dominant over the other.

Of note, the sum of $\Delta\varepsilon$ and $\Delta\varepsilon'$ of the DD model leads to the $\Delta\varepsilon$ value of the CC model for all the samples of Table 1 in the limit of the experimental errors.

The conductivity values of the samples in Table 1 for the three models are very similar, and are in agreement with $\sigma = 0.125\ \Omega^{-1}\,m^{-1}$ at $c = 30$ mM and 25 °C [14], $\sigma = 0.0905\ \Omega^{-1}\,m^{-1}$ at $c = 25$ mM and 25 °C and $\sigma = 0.310\ \Omega^{-1}\,m^{-1}$ at $c = 104$ mM and 25 °C in [16].

The values of σ calculated by Eq. (5) are in good agreement with the data of Table 1 as shown in Fig. 3. Taking into account the hydrodynamic interaction effects (hif) at high concentrations, where strong overlap of the double layers likely occurs, the sigma values have been recalculated as in [35] (Eq. (151)). Results are reported in Fig. 3 (stars). The effect of the hif correction is negligible for the small concentrations, but yields values sensibly smaller than the experimental ones at the highest concentration. This discrepancy can be partially explained, but only to a small amount, by the presence of the low frequency delta relaxation due to the radial motion of counterions that occurs below the low frequency limit of this work.

The ϕ values of each sample for the three models are very similar. The values obtained with the CC and DD models, ϕ_e, are reported in Fig. 4 (triangles and circles) together with the values ϕ_b (black squares) computed from the amount of water added to the surfactant assuming that all water behaves as bulk water. There is a clear disagreement between the two data set, indicating that water cannot be considered wholly as bulk water, but that some bound water, characterized by a lower dielectric constant, must be present in the solution. This is a common finding also in the study of macroscopic charged interfaces [36].

The water volume fraction has been recalculated considering the micelle volume, according to the equation:

$$\phi = 1 - (4/3)\pi R_M^3 N_A (c - \mathrm{cmc})/N. \tag{6}$$

Using for R_M the core radius obtained from SANS data and subtracting the shell thickness $d = 5.5$ Å from the micelle radius R ([26], see Table 2), the values ϕ_c of Fig. 4 have been obtained (squares); using for R_M the full micelle radius R the values ϕ_m are obtained (stars).

A comparison among the ϕ_b, ϕ_c and ϕ_m values clearly shows that there is some water in the system that does not behave as bulk water, we say the water molecules trapped in the interfacial regions. This water differs from bulk in polarizability and relaxation time constant. These findings, in our opinion, show that the DD model gives a better insight into the physics of the micellar interfacial region as also argued in Refs. [8,15,16,30]. Thus in our study the DD model takes into account the relaxation processes due to Grosse's lateral motion and to the bound water reorientation in the interfacial region. Presumably, the CC model, taking into account a spread of single relaxation times, yields a weighted average of these two interfacial relaxations.

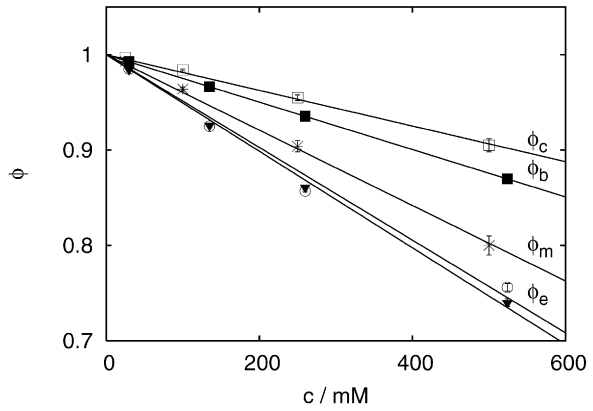

Fig. 4. Volume fraction of water according to different models. Triangles and circles (ϕ_e) are values from the Cole–Cole and the double Debye models, respectively. Stars, black squares and squares are the calculated values ϕ_m, ϕ_b and ϕ_c, respectively, as described in the text.

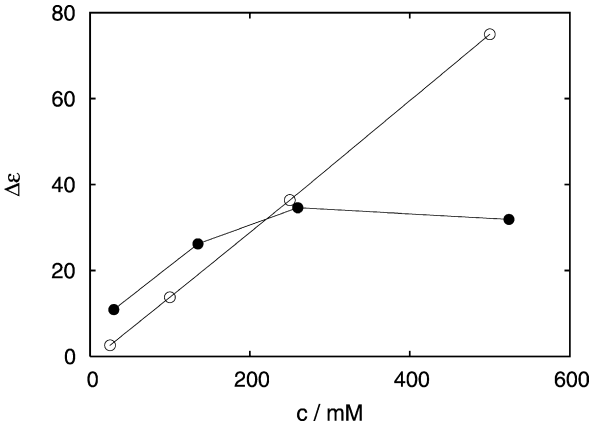

Fig. 5. Experimental $\Delta\varepsilon$ by the double Debye model (black circles) and calculated values by Grosse's model (circles). The lines are guides for the eye. The experimental errors are smaller than symbols.

The number n_w of bound water molecules per surfactant molecule has been computed from data in Fig. 4 taking linear fits of the data and computing $n_w = w_m(\phi_b - \phi_x)/c$, where w_m is the water molarity (55 M), and ϕ_x is ϕ_m or ϕ_e. Results are 14 and 8 water molecules per surfactant molecule respectively, for the experimental ($_e$) and the model ($_m$) data. By comparison, in Ref. [26] the value 10 is reported.

The $\Delta\varepsilon$ and τ values of Table 1 are reported as a function of surfactant concentration in Figs. 5 and 6, to compare our experimental results to Grosse's model [10,13]:

$$\Delta\varepsilon = \frac{9\varphi\varepsilon_m\left(\frac{2\lambda}{R\kappa_m} - \frac{\varepsilon_p}{\varepsilon_m}\right)^2}{\left(\frac{\varepsilon_p}{\varepsilon_m} + 2\right)\left(\frac{2\lambda}{R\kappa_m} + 2\right)^2}, \tag{7}$$

$$\tau = \frac{\varepsilon_o(\varepsilon_p + 2\varepsilon_m)}{\frac{2\lambda}{R} + \kappa_m}, \tag{8}$$

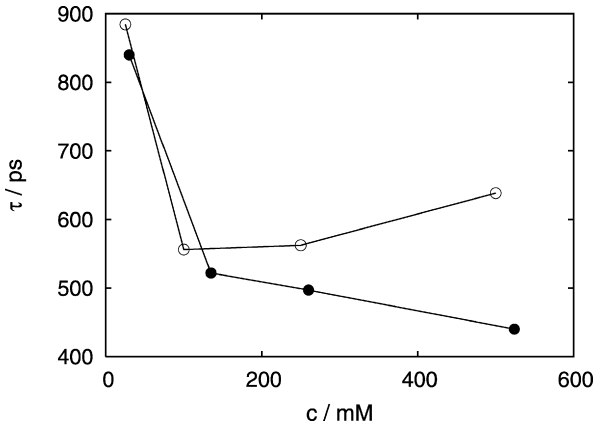

Fig. 6. Experimental τ by the double Debye model (black circles) and calculated values by Grosse's model (circles). The continuous lines are guides for the eye. The experimental errors are smaller than symbols.

where φ is the volume fraction of the micelles ($\varphi = 1 - \phi$), $\varepsilon_p = 2$ is the dielectric constant of the surfactant molecules hydrophobic chains that fill the micellar core as in [14,16] and ε_m is the static permittivity of water. The conductivity of the dispersing medium is $k_m = e^2 N_A (u_{Na^+} + u_{DS^-}) \cdot \text{cmc}$ due to dissociated surfactant molecules. The surface conductivity is

$$\lambda = \frac{e^2 \alpha N}{4\pi k_B T R^2} \cdot D_{Na^+}, \tag{9}$$

where T is the absolute temperature, k_B is the Boltzmann constant and $D_{Na^+} = 1.33 \cdot 10^{-9}\ \text{m}^2\,\text{s}^{-1}$ is the sodium self-diffusion coefficient at infinite dilution [37]. The latter value agrees with the value obtained by molecular dynamic simulation for SDS micellar solutions: D_{Na^+} value has been found to be between $1.0 \cdot 10^{-9}$ and $1.9 \cdot 10^{-9}\ \text{m}^2\,\text{s}^{-1}$, depending on the distance of the ion from the micellar surface [38].

The conditions assumed in Grosse's model are: (a) The interactions among neighboring particles are negligible (the model deals with diluted systems); (b) Debye's length, l_D, is smaller than the radius of the particles.

For SDS at concentration from 0.065 to 0.521 M, studied by SANS, the micelle average radius changes from 22.4 to 25.8 Å, l_D changes from 24 to 13 Å and the micellar surface charge number increases from 13 to 21 [25]. Thus, in the case of our 29.8 mM sample, Debye's length is longer than the micellar radius whereas for 134.9 mM it is comparable with the radius and for 259.9 and 524 mM it is smaller than the radius. As a consequence, the diluted samples should not follow the Grosse model because of the high l_D value; the concentrated samples should not follow the Grosse model because of the strong interactions between neighboring micelles. However from Figs. 5 and 6, it is clear that Grosse's model is in fair agreement with the experimental results at low surfactant concentrations.

From our experimental results we see that the lateral relaxation mode is characterized by a step amplitude $\Delta\varepsilon$ that increases from 11 to 35 with concentration up to 259.9 mM, and remains almost constant up to 524 mM (Fig. 5). From the SANS results [26] it appears that the more concentrated the micellar solution, the greater the surface charge Q of the micelle and the smaller the extension of Debye's length. Thus, more counterions are in the diffuse layer and more frequent are the counterions hops, with a sort of saturation above 259.9 mM. In parallel, τ vs c decreases quickly to half the value from $c = 29.8$ to $c = 134.9$ mM; thereafter τ goes on decreasing slowly above 134.9 mM (Fig. 6). From Table 2 it is clear that the radius does not change very much increasing surfactant concentration, thus the saturation seems due to an increase of interaction among micelles.

The relaxation process due to water trapped in the interfacial region (bound water) is slower than the hydrogen bond network relaxation and leads to a $\Delta\varepsilon'$ value that increases linearly one order of magnitude, from 1.2 to 12.2, over the surfactant concentration range. Correspondingly, τ' decreases from 125 ps to 100 ps. The value $\tau' = 120$ ps is considered typical for bound water in micelles [16,17].

6. Conclusion

The interfacial relaxation processes of SDS micellar solutions were investigated by Dielectric Spectroscopy in the broad concentration range $c = 29.8$–524 mM, explored for the first time above 104 mM. The contribution of the micellized surfactant was analyzed by means of CC and DD models obtaining equivalent χ^2 values; similar relaxation times were obtained for each sample with both models; $\Delta\varepsilon$ of the CC model resulted equal to the sum of $\Delta\varepsilon$ and $\Delta\varepsilon'$ of the DD model for each sample. From these results the CC model seems to sum up two relaxation processes, the more important one being due to the lateral charge hopping of the counterions bound to the micelle surface, or the reorientation of ions pairs. This conclusion was also drawn in Refs. [16,17] for 18–104 mM SDS aqueous micellar solutions. Another important experimental result of this work is the accounting for bound water for each sample using the DD model. On this basis we conclude that the DD model describes the physics of the micellar system better than the CC model. Parameters σ, $\Delta\varepsilon$ and τ as a function of concentration, obtained by the DD model, were compared to theoretical models. Conductivity σ is well described by Kallay's model for each sample. $\Delta\varepsilon$ and τ agree with Grosse's gamma relaxation process for each sample except for the more concentrated ones because of interaction between micelles. The bound water, that results from dielectric spectroscopy data, was computed quantitatively using micellar radius, average aggregation number and interfacial shell thickness from SANS results.

Acknowledgments

Thanks are due to W. Kunz and R. Buchner for helpful discussions and for a preprint of their work. This work was supported by Italian MUR, PRIN2005, INFM, and Ente Cassa di Risparmio di Firenze.

Appendix A. Differential and double differential methods

Measurements have been performed using a Vector Network Analyzer (Anritsu MS4661A) using a new absolute measurement procedure that does not need calibration with liquid standard. The method uses two cells built as coaxial transmission lines, with identical mechanical and electrical characteristics, but for the length, h_s for the shorter cell and h_l for the longer one. The two terminal sections of both cells are completely identical and connected, in turn, to the same ports of the VNA; hence their behavior is described by the same couple of 2×2 cascade scattering matrices [28], say **L** and **R**. The remaining central segments of the two cells, of different length, are characterized by a regular and uniform cross section that ensures a reflectionless propagation, as all deviations from uniformity are contained in the **L** and **R** segments. Hence the central segments are described by two diagonal matrices, $\mathbf{H_s}$ and $\mathbf{H_l}$, that contain only respectively the products $\gamma \cdot h_s$ and $\gamma \cdot h_l$, where γ is the transmission line propagation constant.

Combining the cascade matrices $\mathbf{F_s} = \mathbf{LH_sR}$ and $\mathbf{F_l} = \mathbf{LH_lR}$ of the two complete cells (see [21]) for algebraic details), an expression is obtained that relates the product $\gamma \cdot (h_l - h_s)$ to the scattering parameters S of the two complete cell assemblies as measured by the Vector Network Analyzer.

In the simple differential method, by the knowledge of the mechanically measurable difference $h_l - h_s$, the quantity γ can be computed and from that, under some simplifying assumptions, the complex dielectric constant $\epsilon' - j\epsilon''$ can be obtained.

More accurate results are obtained using the Double Differential Method. The whole measurement procedure is repeated twice, first as described above, then with identical procedure, but with the same cells empty and clean. In this case the product $\gamma_0 \cdot (h_l - h_s)$ is obtained, where γ_0 is the propagation constant for vacuum. Dividing the previous result by this one, the quantity $h_l - h_s$ elides, as well as the contributions of the resistive and inductive components of the transmission line, yielding in the last

$$\left(\frac{\gamma}{\gamma_0}\right)^2 = \epsilon' - j\left(\epsilon'' + \frac{\sigma}{\omega\epsilon_0}\right)$$

with no approximating assumptions.

References

[1] D.O. Shah, Micelles, Microemulsions, and Monolayers, Science and Technology, Marcel Dekker, New York/Basel/Hong Kong, 1998.
[2] W.M. Gelbart, A. Ben-Shaul, D. Roux, Micelles, Membranes, Microemulsions, and Monolayers, Springer-Verlag, New York, 1994.
[3] D. Fennell Evans, H. Wennestrom, The Colloidal Domain where Physics, Chemistry, Biology, and Technology Meet, VHC Publishers, New York/Weinheim/Cambridge, 1994.
[4] R.J. Williams, J.N. Phillips, K.J. Mysels, Trans. Faraday Soc. 51 (1955) 728.
[5] R.J. Hunter, Foundation of Colloid Science, Clarendon Press, Oxford, England, 1987, p. 332.
[6] T. Shikata, S. Imai, Langmuir 98 (1998) 6804.
[7] S. Imai, M. Shiokawa, T. Shikate, J. Phys. Chem. B 105 (2001) 4495.
[8] C. Baar, R. Buchner, W. Kunz, J. Phys. Chem. B 105 (2001) 2914.
[9] C. Grosse, K.R. Foster, J. Phys. Chem. 91 (1987) 6415.
[10] C. Grosse, J. Phys. Chem. 92 (1988) 3905.
[11] G.J. Schwarz, J. Phys. Chem. 66 (1962) 2636.
[12] H. Pauly, H.P. Schwan, Z. Naturforch. B 14 (1959) 125.
[13] C. Grosse, in: A.T. Hubbard (Ed.), Encyclopedia of Surface and Colloid Science, Dekker, New York, 2002, p. 1404.
[14] R. Barchini, R. Pottel, J. Phys. Chem. 98 (1994) 7800.
[15] C. Baar, R. Buchner, W. Kunz, J. Phys. Chem. B 105 (2001) 2906.
[16] P. Fernandez, S. Schödle, R. Buchner, W. Kunz, Chem. Phys. Chem. 4 (2003) 101.
[17] R. Buchner, C. Baar, P. Fernandez, S. Schrodle, W. Kunz, J. Mol. Liq. 118 (2005) 179.
[18] F. Kremer, A. Schonhals, Broadband Dielectric Spectroscopy, Springer-Verlag, Berlin/Heidelberg, 2003.
[19] L. Lanzi, M. Carlà, C.M.C. Gambi, L. Lanzi, The physics of complex systems—New advances and perspectives, in: F. Mallamace, H.E. Stanley (Eds.), Proceedings of the International School of Physics Enrico Fermi, vol. 155, Distributed by IOS, Amsterdam, 2004, p. 507.
[20] L. Lanzi, M. Carlà, C.M.C. Gambi, L. Lanzi, J. Non-Cryst. Solids 351 (2005) 2864.
[21] L. Lanzi, M. Carlà, C.M.C. Gambi, L. Lanzi, Rev. Sci. Instrum. 73 (2002) 3085.
[22] L. Lanzi, Study of Dynamic and Structural Properties of Self-Assembling Nanoparticles by Dielectric Spectroscopy, Ph.D. thesis, 2006.
[23] J.B. Hayter, J. Penfold, J. Chem. Soc. Faraday Trans. 77 (1981) 1851.
[24] J.B. Hayter, J. Penfold, Colloid Polym. Sci. 261 (1983) 1022.
[25] E.Y. Sheu, C.-F. Wu, S.-H. Chen, Phys. Rev. A 32 (1985) 3807RC.
[26] K.A. Payne, L.J. Magid, D.F. Evans, Prog. Colloid Polym. Sci. 73 (1987) 10.
[27] S.-H. Chen, E.Y. Sheu, Micellar Solutions and Microemulsions, Springer-Verlag, New York, USA, 1990, p. 3.
[28] L.J. Giacoletto, Electronic Designer's Handbook, McGraw–Hill, New York, 1977.
[29] R. Buchner, J. Barthel, J. Stauber, Chem. Phys. Lett. 306 (1999) 57.
[30] R. Buchner, G.T. Hefter, P.M. May, J. Phys. Chem. A 103 (1999) 1.
[31] C.J.F. Bottcher, Bordewijk, Theory of Electric Polarization, vol. II, Elsevier Scientific Publishing, Amsterdam/Oxford/New York, 1980.
[32] N. Kallay, V. Tomisic, V. Hrust, R. Pieri, A. Chittofrati, Colloids Surf. 222 (2003) 95.
[33] R.C. Weast (Ed.), Handbook of Chemistry and Physics, 70th ed., CRC Press, Florida, 1989–1990.
[34] G.D. Parfitt, A.L. Smith, J. Phys. Chem. 60 (1962) 942.
[35] E.K. Zholkovskiy, V.N. Shilov, J.H. Masliyah, M.P. Bondarenko, Can. J. Chem. Eng. 85 (2007) 701.
[36] J.O'M. Bocris, A.K.N. Reddy, Modern Electrochemistry, Plenum Press, New York, 1970, p. 756.
[37] Y. Marcus, Ion Properties, Marcel Dekker, New York/Basel/Hong Kong, 1997.
[38] C.D. Bruce, M.L. Berkowitz, L. Perera, M.D.E. Forbes, J. Phys. Chem. B 106 (2002) 3788.